Rational Design and Investigation of Nonlinear Optical Response Properties of Pyrrolopyrrole Aza-BODIPY-Based Novel Push-Pull Chromophores

Naga Pranava Sree Kothoori[1], Pandiyan Sivasakthi[1], Mallesham Baithy[1], Ramprasad Misra[2,*], and Pralok K. Samanta[1,3,*]

[1]*Department of Chemistry, School of Science, Gandhi Institute of Technology and Management (GITAM), Hyderabad-502329, India*

[2]*Institute for Biology, Experimental Biophysics, Humboldt-Universität zu Berlin, Berlin-10115, Germany*

[3]*Department of Chemistry, Birla Institute of Technology and Science (BITS) Pilani, Hyderabad Campus, Hyderabad-500078, India*

Abstract

Intramolecular charge transfer (ICT)-based chromophores are highly sought for designing near-Infrared (NIR) absorbing and emitting dyes, as well as designing chromophores for nonlinear optical (NLO) applications. The properties of these so-called 'push-pull' molecules could be tuned easily through modification of the electronic donor (D) and acceptor (A) groups as well as by the π-conjugating linker. This study presents rational design and quantum chemical investigation of the correlation between the structural attributes, electro-optical properties, and NLO characteristics of molecules with a D–π–A framework for applications in photonics. The one- and two-photon absorption (2PA), average linear polarizability (α_{av}) as well as the first hyperpolarizability (β) of novel chromophores consisting of a Dimeric aza-Boron Dipyrromethene (aza-BODIPY) analogue known as pyrrolopyrrole aza-BODIPY (PPAB) as acceptor and Triphenylamine (TPA) or Diphenylamine (DPA) as electronic donor with thienyl or phenylene groups as linkers are studied. Additionally, the Hyper-Rayleigh Scattering (β_{HRS}) which enables to directly estimate the second-order NLO properties is also calculated for these compounds with 1064 nm excitation in Acetonitrile solvent. Significant increase in the β with increasing solvent polarity indicates the role of ICT in shaping NLO response of these molecules. The two-photon absorption cross-section of studied molecules could also be enhanced through modulation of donor and linker combinations. Our findings show that the D–π–A molecules designed in the present work exhibit significantly larger hyperpolarizabilities values, compared to the standard p-Nitroaniline, making them suitable candidates for future NLO applications.

*Corresponding authors: ramprasad.misra@hu-berlin.de (RM); pralokkumar.samanta@hyderabad.bits-pilani.ac.in (PKS)

1. Introduction

Nonlinear optical (NLO) materials are crucial for the development of contemporary technologies, including communications, signal processing, and data storage.[1–4] Materials possessing optical limiting (OL) qualities have the ability to effectively absorb significant amounts of high-energy lasers, hence reducing the output energy plays an important role in safeguarding human eyes and optical systems against laser-induced harm.[5,6] The demand for designing of new NLO materials has significantly increased in the field of optoelectronics and photonics in recent years. The captivating photo-physical properties exhibited by NLO materials under intense laser irradiation account for their extensive range of practical uses. Organic compounds are highly sought after for designing novel NLO materials, owing to their capability to achieve rapid response rates, increased photo-electric quantum efficiency, low dielectric constants.[7] Organic molecules also possess greater design freedom in comparison to inorganic substances, rendering them more economically efficient, compared to their inorganic counterparts.[8] In order for a molecule to demonstrate NLO characteristics, it must contain a significant initial hyperpolarizability and non-Centrosymmetric geometry.[9,10] Organic chromophores that display strong absorption and emission in the near-infrared (NIR) region are useful for several technological applications, including, solar cells, heat absorbers and NIR-emitting diodes.[11] BODIPY molecules possess notable absorption properties and demonstrate highly efficient fluorescence emission in this range of NIR wavelength.[12] The absorption and emission characteristics of these molecules can be readily altered by changing the substitution pattern of the BODIPY framework, leading to an increase in their fluorescence in the NIR spectrum.[13] These dyes are well-known for their remarkable resistance to heat and light-induced chemical reactions, and their capacity to produce fluorescent sensors.[14] PPAB (see **Figure 1**) was shown to possess a wide absorption spectrum in the visible and near-infrared ranges, which can be attributed to its extensive conjugate structure.[15] In biological assays and screening procedures, dyes that have NIR absorption and emission properties are favoured because they experience less interference from auto fluorescence and have a greater ability to penetrate deeper into the sample.[16,17] Of late, intramolecular charge transfer (ICT)- based molecules with electron-donating and electron-accepting components, connected either alone or via π-linkers are popular for designing chromophores for NLO materials.. Incorporating suitable electronic donor (D) and acceptor (A) components on opposing sides of the π-linker, for example, molecules with D–

A, D-π-A, D–A–D, and A–D–A architectures, can lead to a high second-order NLO response.[18–21]

Recently, Wang *et al* reported a series of molecules with donor-acceptor-donor (D–π–A– π–D) framework with the Pyrrolopyrrole aza-BODIPYs as the acceptor moiety with Triphenylamine (TPA) or Diphenylamine (DPA) as donors, with thienyl or phenylene linker.[22] They studied the singlet emission properties of these molecules, which was observed at NIR region. In this study, we investigated the absorption and NLO response properties of aforesaid molecules with (D–π–A–π–D) structure, which led us to design molecules with D–π–A architecture for obtaining chromophores for higher NLO response. The PPAB core present in all three compounds (**Figure 2**), and these molecules demonstrate a high level of resistance to degradation caused by light which is a phenomenon usually exhibited by inorganic framework containing NLO molecules.[23] The π-conjugation bridge, which is in this case a thienyl or phenylene linker, promotes ICT.[24,25] A π-conjugated linker is employed to establish a connection between both the electron-donating and electron-withdrawing groups in a molecule. This process leads to an improvement in the NLO properties of the molecules. Varying the nature of the donor groups and the π-conjugated bridge by means of chemical design is the most common strategy for tuning of the first hyperpolarizability (β_{tot}). We also studied the second-order NLO properties of the PPAB molecules which form the basis for the designing of the NLO switching, among others. Imaging using two-photon absorption (2PA) produced photoluminescence is reported to be more advantageous than one-photon induced photoluminescence due to its ability to provide three-dimensional resolution.[26] Additionally, when excitation is conducted in the NIR range, it enables greater penetration depth.[27,28] The PPAB cored molecules exhibit strong performance in the NIR range, with 2PA cross sections of approximately 3000 GM at the telecommunication window at a wavelength of around 1500- 1700 nm.[29]

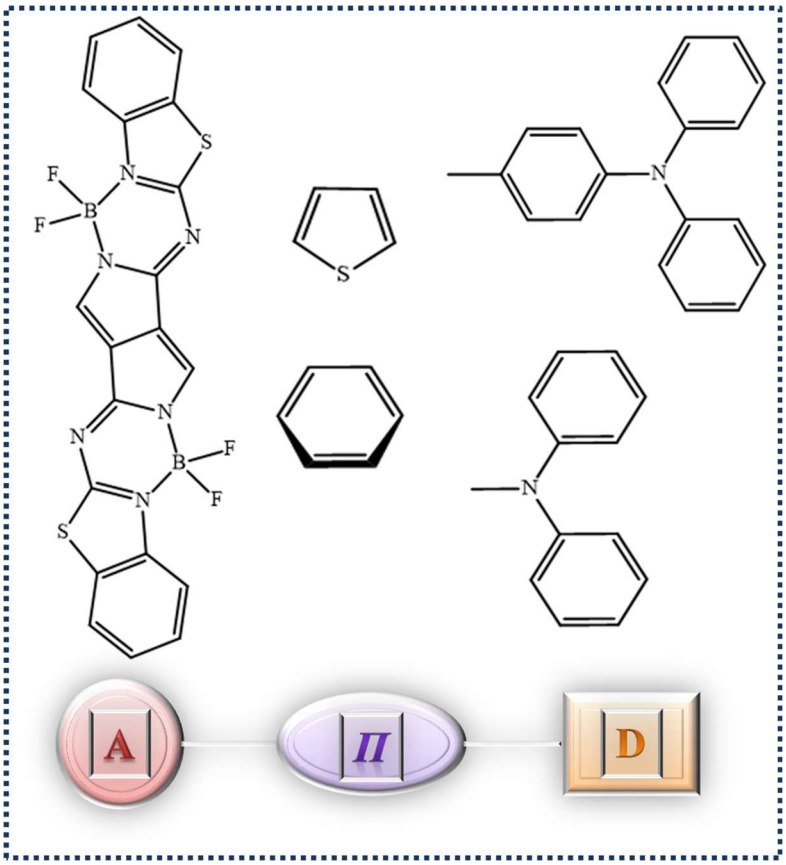

Figure 1. The 2-D representation of the acceptor, linker, and donor components.

2. COMPUTATIONAL DETAILS

The optimization of the ground state geometries were done using the Density functional theory (DFT) with range-separate parameter (ω) tuned ω*B97XD functional and 6-31G* basis set. The optimized ω values were estimated by minimizing J^2 as follows:[30,31]

$$J^2 = \sum_{i=0}^{1} |\varepsilon_H(N+i) + IP(N+i)|^2 \quad (1)$$

Where IP and ε_H are the ionization potential and HOMO energy of a given molecule, respectively, and N is the total number of electrons in the molecule. Absorption spectra are obtained by implementation of time-dependent DFT (TDDFT) methods. All the computational calculations were done using the Gaussian 16 program.[32] The absorption and NLO response of the molecules are studied in three solvents with varying polarity namely, Acetonitrile, Chloroform and Toluene. The highly polar solvent acetonitrile is selected to study the dynamic NLO properties of the studied molecules. The polarizable continuum model (PCM) in the framework of the self-consistent reaction field (SCRF) has been used to mimic the presence of solvent.[33] Several properties following the geometry optimization of the molecules such as the dipole moment, average polarizability and first hyperpolarizability

of the chromophores were studied. The calculation of the dipole moment of the molecules is calculated using the **Equation 2**.

$$\mu = (\mu_x^2 + \mu_y^2 + \mu_z^2)^{1/2} \quad (2)$$

In the above equation, *x, y* and *z* denote the direction and the μ_x, μ_y, μ_z are the dipole moment components of the molecule.[34] The frontier molecular orbital (FMO) images, including, the highest occupied molecular orbital (HOMO) and the lowest unoccupied molecular orbital (LUMO) are analyzed to estimate the band gap in the molecules and also to obtain global reactivity indices. Visual molecular dynamics (VMD) is used to analyze and visualize the FMOs.[35] The percentage of CT and local excitation (LE) in a transition between the lowest excited singlet and triplet state are calculated via inter fragment charge transfer method using Multiwfn code.[36] The 2PA calculations were done using B3LYP functional and 6-31G* basis set for the ω*B97XD optimized coordinates using DALTON software.[37]

3 RESULTS AND DISCUSSION

3.1(a) Comparison between push–pull dipolar and quadrupolar chromophores

As molecules with emission properties in the NIR region are highly intriguing, we examined the NLO response of molecules (1-3) with D–π–A–π–D architecture (**Figure 2**).[22] The ground state geometry of these molecules were optimized, followed by computation of their first hyperpolarizability. Before computing their NLO response properties, the one-photon absorption of these molecules were studied using time-dependent density functional theory (TDDFT)to find out the best basis set/functional combination. Several functional including B3LYP, PBE1PBE, CAM-B3LYP, ωB97XD, and ω*B97XD, with a 6-31G(d) basis set were used to study the absorption of the aforesaid molecules (**Table 1 and S1**). Our analysis revealed that the tuned functional exhibited minimal divergence from the experimental absorption values. As the NLO properties of quadrupolar molecules with D–π–A π–D framework were not much satisfying (see **Table S2 and S3)**, presumably due to their Centro-symmetric nature**,** basic molecular structure modifications to D–π–A were made, which helped us to greatly enhance the NLO response of the molecules.

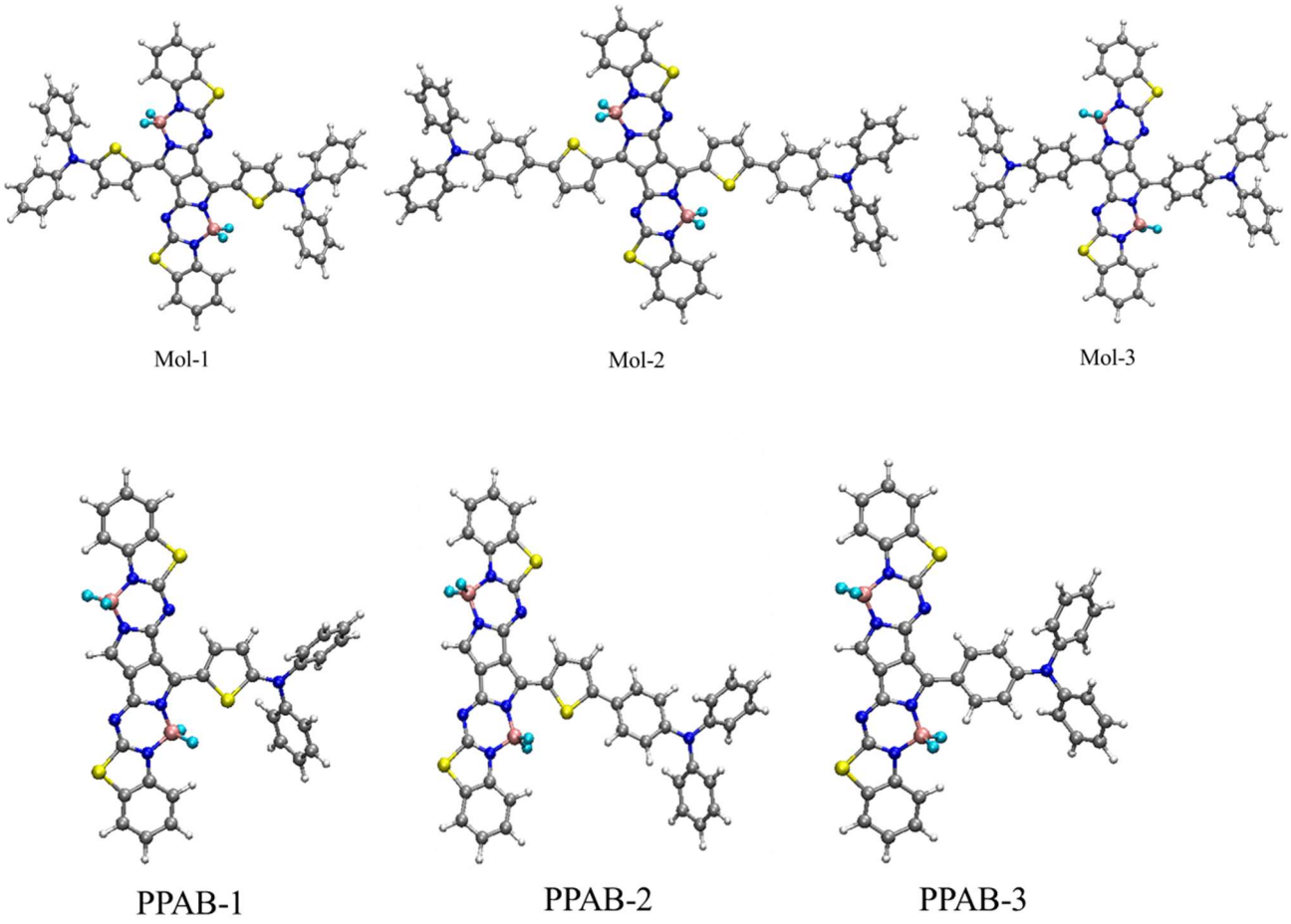

Figure 2. Design strategy of novel PPAB chromophores for NLO applications: Upper panel shows the optimized geometries of D–π–A-π–D series of molecules (1-3), used earlier for designing NIR-emitting dyes [Ref. 22]. As NLO response of these molecules are quite low, presumably due to their centrosymmetric nature, using the same donor and acceptor groups we have designed D–π–A chromophores PPAB (1-3), whose optimized geometries are shown in the lower panel.

Table 1. Calculation of one-photon absorption energy (λ_{abs}) with different DFT functionals. The experimental values are obtained from [Ref. 22]. All values are provided in nm.

Molecules	[22]Expt.	ω*B97XD	ωB97XD	CAM-B3LYP	B3LYP	PBE1PBE
Mol-1	816	752.19	690.15	701.15	792.21	769.86
Mol-2	797	727.47	654.85	671.09	855.07	808.79
Mol-3	728	692.47	611.63	626.46	776.61	743.25

3.1(b) Geometrical Structure optimization of PPAB Molecules in the ground state

By taking the D–π–A π–D as the basis the electronic structure calculations for the D–π–A molecules were performed using (ω*B97XD) functional and 6-31G (d) basis set and the ground state optimized geometries of the molecules PPAB(1-3) are shown in **Figure 2**. The absence of imaginary frequencies in the vibrational frequency analysis indicates that the optimised geometries have reached at least one of their local minima. In the present work, we theoretically studied the molecules with D–π–A structures in which the PPAB acts as an electron acceptor, TPA and DPA act as electron donor and the thienyl or phenylene molecules which can be π-conjugated linker.

3.2 Charge transfer (CT) and Locally excited (LE) characteristics.

The ICT is an important factor which affects the NLO properties of organic molecules. Among the PPAB chromophores, PPAB-2 show higher percentage of CT character which results in higher β_{tot} values, owing to the Thienyl group which is a typical electron-rich substituent. Therefore, the introduction of thienyl as bridge between the A–D is beneficial to enhance the ICT which provides a large transition dipole moment, which can strongly affect the polarizability of the molecule. The tendency to engage in ICT from TPA or DPA to PPAB and moieties, facilitated by suitable π-linkers, is a significant factor in understanding the structure-function relation for designing of NLO materials. It is known that a strong electron 'push-pull' effect has a positive influence on the NLO performance of molecules, and a high electron-donating capacity in a molecule with D−π–A architecture benefits the ICT. Consequently, the electron donating group of PPAB-2 has a greater capacity to donate electrons compared to PPAB-1. This results in a higher ICT (intramolecular charge transfer) character. The higher ICT character is achieved by replacing the DPA (donor group) with TPA (donor group) in the structure.

3.3 Solvent effect on one-photon absorption

The calculation of the one photon absorption energies, oscillator strength (*f*) and the fluorescence emission of PPAB (1-3) molecules are performed using the TDDFT method. As the change in solvent polarity is likely to result in a substantial alteration of the optical characteristics of ICT-based molecules[38], we go beyond gas-phase calculations to investigate the impact of a continuum dielectric on the electronic structure and properties, such as, dipole moment (μ), average polarizability (α_{avg}), and first hyperpolarizability (β) of the PPAB chromophores. The UV-visible absorption spectra was analysed in solvents with different polarities, namely Acetonitrile, Chloroform, and Toluene. The absorption values are tabulated

in **Table 2**. All the studied molecules exhibit considerable absorption with high oscillator strength within the purple light wavelength range. For example, PPAB-1, PPAB-2, and PPAB-3 exhibit maximal absorption peaks at wavelengths of 579 nm, 643 nm, and 611 nm, respectively, in Acetonitrile. The emission from the lowest excited singlet stated (S_1), also known as fluorescence emission, which is calculated for PPAB 1, 2, and 3 in Acetonitrile are observed at wavelengths of 678 nm, 738 nm, and 674 nm, respectively. The notably high Stokes shift also indicate the CT nature of the studied molecules.

Table 2. The one-photon absorption wavelength (eV) with oscillator strength (*f*) and dominant orbital transition(s) and fluorescence emission details, as obtained using TDDFT calculations employing ω*B97XD functional and 6-31g* basis set in different solvents.

Molecules	Solvent Medium	λ_{abs} ($S_0 \rightarrow S_1$) in eV	Dominant Transition	λ_F ($S_1 \rightarrow S_0$) in eV
PPAB-1	Acetonitrile	2.01 (*f*=0.91)	H→L (98.10%)	1.83 (*f*=1.31)
	Chloroform	1.98 (*f*=0.95)	H→L (98%)	1.93 (*f*=1.31)
	Toluene	1.97 (*f*=0.97)	H→L (97.96%)	2.02 (*f*=1.29)
PPAB-2	Acetonitrile	1.93 (*f*=1.18)	H→L (78.2%), [H-1]→L (17.6%)	1.68 (*f*=1.71)
	Chloroform	1.93 (*f*=1.2)	H→L (76.8%), [H-1]→L (19.2%)	1.81 (*f*=1.7)
	Toluene	1.93 (*f*=1.20)	H→L (76.56%), [H-1] →L (19.69%)	1.92 (*f*=1.68)
PPAB-3	Acetonitrile	2.03 (*f*=0.81)	H→L (93.9%), [H-1] →L (3.1%)	1.84 (*f*=1.11)
	Chloroform	2.01 (*f*=0.85)	H→L (93.51%), [H-1] →L (3.53%)	1.93 (*f*=1.03)
	Toluene	2.0 (*f*=0.87)	H→L (93.4%), [H-1] →L (3.7%)	2.0 (*f*=0.88)

3.4 Frontier molecular orbital (FMO) Analysis

To understand the nature of the studied chromophores, we have analysed the parameters including, the HOMO-LUMO energy gap and percentage of CT and LE characters of the excited state. The assessment of the FMO, including, the HOMO-LUMO energy gap is crucial for understanding the structure-function relationships of molecules with ICT nature. To explore the distribution patterns of molecular orbitals of HOMO and LUMO, we examined the FMO of the PPAB molecules in Acetonitrile solvent using the polarizable

continuum model, as illustrated in **Figure 3**. It is clear based on the FMO analysis that the HOMO densities of all PPAB molecules exhibit similarity as they are distributed over the donor moiety, indicating a π-bonding nature and the LUMO densities are dependent upon the electron-withdrawing moieties, exhibiting a π-antibonding nature. The chemical stability, electrical, and optical characteristics of molecules are also reportedly correlated well using FMO analysis.[39] Compounds with a lower HOMO–LUMO energy gap have higher chemical reactivity, and these compounds are highly polarizable, showing excellent NLO properties because of higher possibility of ICT.[40] The FMO analysis is done in three solvents with different polarity as well to study the effect of polar solvent on the HOMO-LUMO energy gap. Furthermore, energy gaps (ΔE_{HL}) of the HOMO to the LUMO are shown in **Table 3**. The ΔE_{HL} value of PPAB-2 (3.869 eV) is lower than that of PPAB-1and PPAB-3, thus the molecules possessing planarity and a low energy gap (ΔE) showed better NLO response. The molecule with low energy gap have high softness value and low hardness value. The ionization potential (IP), global electron affinity (EA), chemical hardness (η), chemical softness (σ) are calculated using the following equations.[41–43]

$$IP = -E_{HOMO} \tag{3}$$

$$EA = -E_{LUMO} \tag{4}$$

$$\eta = \frac{[IP-EA]}{2} \tag{5}$$

$$\sigma = \frac{1}{2\eta} \tag{6}$$

Table 3. The values of ΔE_{HL} (in eV) are obtained using ω*B97XD/6-31G* functional and basis set for the ground state PPAB molecules along with the CT and LE percentage. Global reactivity parameters of PPAB molecules are also reported, which are in Hartree.

Molecules	HOMO (eV)	LUMO (eV)	ΔE_{HL} (eV)	CT (%)	LE (%)	*IP*	*EA*	*η*	*σ*
						in Hatree			
PPAB-1	-6.286	-2.090	4.196	47.2	52.8	0.231	0.077	0.077	6.493
PPAB-2	-6.210	-2.341	3.869	56.9	43.1	0.228	0.086	0.071	7.042
PPAB-3	-6.402	-2.227	4.175	50.1	49.9	0.235	0.082	0.076	6.579

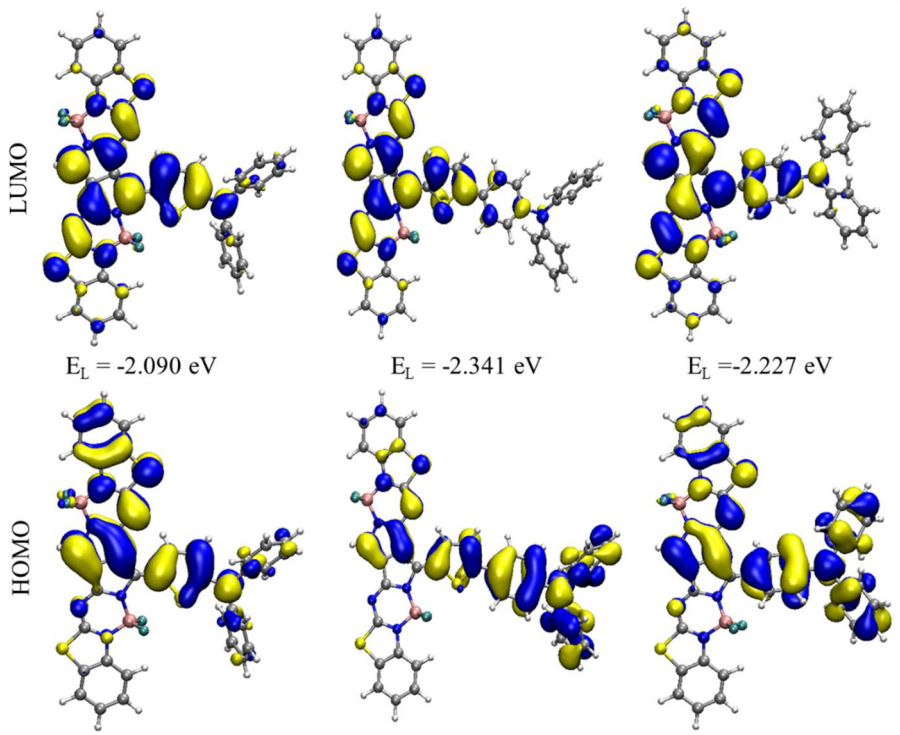

Figure 3. The HOMO and LUMO images with the energies of the D−π–A molecules, PPAB (1-3) in the PCM Model corresponding to Acetonitrile solvent.

3.5 Electrostatic Potential Calculations

The study of the electrostatic potential (ESP) provides a perceptive understanding of the distribution of charges within the molecule (see **Figure 4**). The ESP of aza-BODIPY molecules containing DPA and TPA groups exhibit significant differences. The region with a more negative potential, is denoted by red regions, is predominantly situated on the F atoms of the aza-BODIPY group. However, the DPA and TPA group exhibits a net positive potential, indicated by blue regions. This observation suggests that the aza-BODIPY group acts as the electron-acceptor group, while the DPA and TPA group serves as the electron-donor group which results in ICT which play a major role in NLO properties of the molecule.

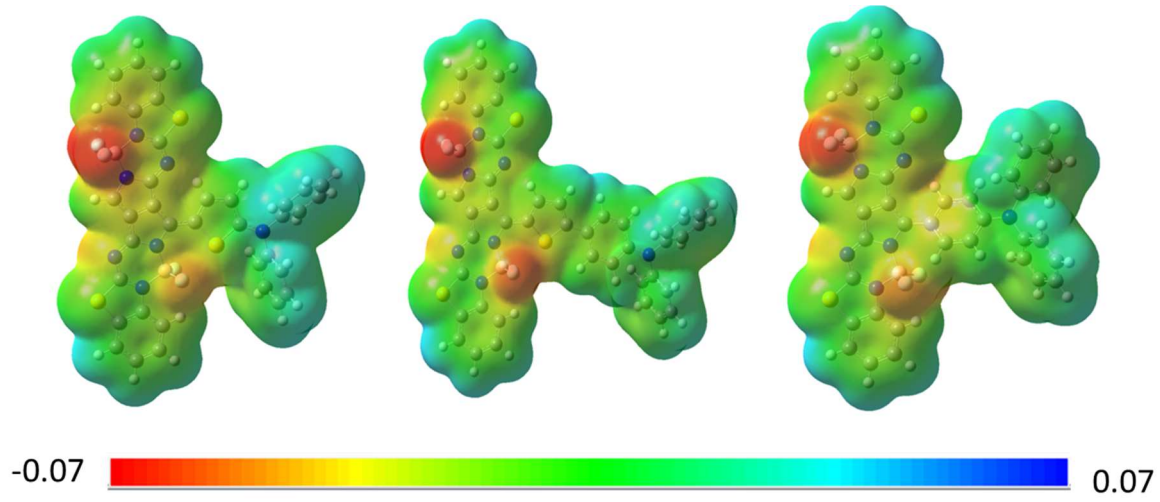

Figure 4. The Electrostatic potential (ESP) of D–π–A molecules. The potential distribution in the ESP map increase in the order red < yellow < green < blue. The range of ESP map is ranging from -0.07 a.u. to 0.07 a.u.

3.6 Dipole moment (μ), average polarizability (α_{av}) and first-order hyperpolarizability (β)

The Dipole moment, average polarizbility and first hyperpolarizability of PPAB (1-3) are computed in the Acetonitrile, Chloroform and Toluene are reported in the **Table 4**. The important factors that affect the NLO properties in these molecules are also discussed.[44] Higher values of μ indicate higher polarity of the molecule in the ground state. The first hyperpolarizability (β) is a second order NLO property, which can be tuned by using strong electron donor and acceptor groups, HOMO and LUMO energy gap, high difference of μ between the ground and excited states. In general, the extend of CT of a molecule play a major role in obtaining high β values. The μ values of PPAB-1, PPAB-2 and PPAB-3 are higher in more polar solvent acetonitrile with their values of 13.834 D, 9.06 D and 7.32 D, respectively. This indicates that PPAB-1 consists of a low-lying excited state with stronger charge transfer (CT) compared to PPAB-2 and PPAB-3. p-nitroaniline is a well-known D–π–A model molecule that has gained a lot of attention from both experimentalists and theorists.[45] The NLO properties of p-nitroaniline is also calculated using ω*B97XD/6-31G* functional and basis set to compare its results with PPAB- D-π-A structures (see **Table 4)**. The components of linear polarizability appear in the Gaussiaon16 output as follows: α_{xx}, α_{xy}, α_{yy}, α_{xz}, α_{yz} and α_{zz}. The average polarizability (α) is a second rank tensor, which is calculated by the given following **Equation 7**.

$$\propto_{av} = \frac{(\propto_{xx} + \propto_{yy} + \propto_{zz})}{3} \quad (7)$$

The static first order hyperpolarizability,(β_{tot}) is a third rank tensor[46] with twenty seven components which can be reduced to ten components by virtue of Kleinman symmetry.[47] Those ten components are β_{xxx}, β_{xxy}, β_{xyy}, β_{yyy}, β_{xxz}, β_{xyz}, β_{yyz} , β_{xzz},β_{yzz} and β_{zzz} of the (3 × 3 × 3) tensor. These components have been used to define β_{vector} which is projected in the direction of the dipole moment of the molecule, as well as the β_{tot} which is computed by using the **Equation 8**.

$$\beta_{tot} = \sqrt{(\beta_{xxx} + \beta_{xyy} + \beta_{xzz})^2 + (\beta_{xxy} + \beta_{yyy} + \beta_{yzz})^2 + (\beta_{xxz} + \beta_{zyy} + \beta_{zzz})^2} \quad (8)$$

The β_{tot} and vector component of first hyperpolarizability (β_{vec}) of molecules are obtained by using the tuned functional. The β_{vec} at the static limit is calculated using the equation 9.

$$\beta_{vec} = \frac{(\beta_x \mu_x + \beta_y \mu_y + \beta_z \mu_z)}{\mu} \quad (9)$$

The ratio of β_{vec} and β_{total} is known to provide crucial information about the direction of charge transfer in an ICT-based molecule.[48] Unidirectional charge transfer, indicated by ratio of β_{vec} and β_{total} of unity, could be used to enhance the NLO response of a molecule.

Among the molecules studies, PPAB-2 showed the highest β_{tot} value, while PPAB-1 showed the lowest β_{tot} value. The higher β_{tot} of PPAB-3 than the PPAB-1 could be assigned to the unidirectional charge transfer in the former, as indicated by the ratio of β_{tot} to β_{vec} close to unity. The β_{tot} of the three molecules are investigated in different solvents in which the results clearly indicate that the inclusion of the solvation effect leads to a substantial increase in the β_{tot} values of the compounds under investigation. As the extend of ICT is known to enhance with increasing solvent polarity, we can infer that the ICT plays a significant role in shaping the NLO response of the PPAB (1-3).[49] The β_{tot} value of the molecules in acetonitrile solvent is much higher compared to the values observed in the less polar solvents. This finding suggests that the presence of a polarizable environment can effectively modulate the NLO response. The increase in β by modifying the dielectric environment around the chromophore is a potential method to greatly improve the performance of nonlinear optical systems. The components of the μ as well as that of β are provided in **Table 5**. The results indicate that unlike PPAB-1, the hyperpolarizability of PPAB-3 dominated by only one component (β_y), indicating unidirectional charge transfer in the later. Therefore, these results indicate that the β values of the PPAB molecules can be tuned using suitable donor and acceptor groups that facilitates unidirectional charge transfer.

Table 4. The values of dipole moment (μ), average polarizability (α_{av}) and β_{total} for molecules PPAB (1-3) in Acetonitrile, Chloroform, Toluene, as obtained using DFT calculations employing ω*B97XD functional and 6-31g* basis set. The same properties computed for the reference molecule p-nitroaniline in Chloroform is reported for comparison.

Molecules	Solvent	μ (in Debye)	α_{av} (in a.u.)	β_{tot} (in a.u.)	β_{vec} (in a.u.)	β_{vec}/β_{tot}	β_{HRS} in 1064 nm
PPAB-1	Acetonitrile	13.834	975.29	30756.93	-2373.01	-0.08	62071.27
	Chloroform	12.22	893.68	22857.57	-5559.25	-0.24	
	Toluene	10.90	824.96	17492.15	-6582.11	-0.38	
PPAB-2	Acetonitrile	9.06	1168.80	144576.99	-141783.9	-0.98	625365.6
	Chloroform	8.352	1060.43	105406.29	-103300.95	-0.98	
	Toluene	7.74	973.75	79374.30	-77810.69	-0.98	
PPAB-3	Acetonitrile	7.32	973.71	58277.21	-54095.37	-0.93	145843.7
	Chloroform	6.76	889.35	45283.05	-42349.34	-0.93	
	Toluene	6.25	600.38	35303.46	-33245.92	-0.94	
p-nitroaniline	Chloroform	8.25	97.88	2211.76	-2190.31	-0.99	-

Table 5. The components of dipole moment (μ) and first hyperpolarizability (β) of molecules PPAB (1–3), obtained using DFT calculations employing ω*B97XD functional and 6-31g* basis set. The same properties computed for the reference molecule p-nitroaniline in Chloroform is reported for comparison.

Molecules	Medium	μ_x	μ_y	μ_z	β_x	β_y	β_z
		in Static					
PPAB-1	Acetonitrile	-3.84	3.85	0.01	-20038.21	-23331.91	-283.63
	Chloroform	3.38	3.42	-0.02	11863.26	-19535.74	293.99
	Toluene	-2.99	3.07	0.04	-7023.23	-16017.20	-314.09
PPAB-2	Acetonitrile	3.55	-0.37	-0.06	-138144.82	42625.39	-1261.99
	Chloroform	3.27	-0.33	0.005	-100709.30	31093.47	-1149.007
	Toluene	3.03	-0.31	0.03	-75820.65	23465.11	-946.91
PPAB-3	Acetonitrile	0.87	2.74	-0.08	4222.91	-58120.53	635.45
	Chloroform	0.87	2.51	0.08	1344.11	-45260.33	501.31
	Toluene	0.79	2.33	-0.07	600.38	-35296.31	379.53
p-nitroaniline	Chloroform	0.37	-3.23	0.00	56.39	2211.04	2.43

3.7 Dynamic first-order hyperpolarizability

Hyper-Rayleigh scattering (HRS) or the second harmonic Rayleigh scattering(SHLS) is a phenomenon in which light is scattered at harmonic frequencies of the incident light.[50] It is an incoherent nonlinear optical process**.** It is important to take into account the effects of frequency dispersion correction in theoretical calculations because the hyperpolarizability obtained experimentally is under dynamic settings.[51] To make our results useful for the experimentalists and theoreticians alike, frequency dependent NLO response in terms of the β_{HRS} β (−2ω,ω,ω) is calculated.[52] The β_{HRS} is an alternative to electric-field-induced second harmonic generation (EFISHG) for directly measuring the β value of all molecules, regardless of their symmetry or charge. The efficiency of SHG for a molecule is primarily determined by the molecular second-order nonlinear polarizability, or first hyperpolarizability, β. Castet *et al.* devised a method to assess the HRS response β_{HRS} (-2ω; ω; ω) effectively.[53]

The dynamic values used in this study were derived using an incident infrared wavelength (λ) of 1064 nm, which is typical of Nd: YAG laser. Second-harmonic hyperpolarizability β(−2ω,ω,ω) can be measured in solution using hyper-Rayleigh scattering where ω is the frequency of the light field.[54,55] The β_{HRS} hyperpolrizabilities of the molecules is calculated in Acetonitrile. The second-order NLO susceptibility X_{lmn} is a third-rank tensor and the presence of inversion symmetry of the molecule will make X_{lmn}= 0. In this context, molecules with inversion symmetry are not SHG active. The $\beta_{HRS}(-2\omega, \omega, \omega)$ can be described by the equation 10. The computed dynamic β_{HRS} (au) values at the *ω*B97XD/6-31g* level using 1064 nm incident wavelength in Acetonitrile are reported in **Table 4**.

$$\beta_{HRS}(-2\omega, \omega, \omega) = \sqrt{\langle\beta_{ZZZ}^2\rangle + \langle\beta_{ZXX}^2\rangle} \quad (10)$$

The $\beta_{HRS}(-2\omega, \omega, \omega)$ is the sum of $\langle\beta_{ZZZ}^2\rangle$ and $\langle\beta_{ZXX}^2\rangle$ which are the average orientation of the molecular β tensor components. Where the x,y,z are the axis of the molecular frame

The values of the $\langle\beta_{ZZZ}^2\rangle$ and $\langle\beta_{ZXX}^2\rangle$ tensors are calculated by the below **Equations 11** and **12**.

$$\langle\beta_{ZZZ}^2\rangle = \frac{1}{7}\sum_{l}^{x,y,z}\beta_{lll}^2 + \frac{4}{35}\sum_{l\neq m}^{x,y,z}\beta_{llm}^2 + \frac{2}{35}\sum_{l\neq m}^{x,y,z}\beta_{llm}\beta_{lmm} + \frac{4}{35}\sum_{l\neq m}^{x,y,z}\beta_{mll}\beta_{llm}$$

$$+\frac{4}{35}\sum_{l\neq m}^{x,y,z}\beta_{lll}\beta_{mll}+\frac{1}{35}\sum_{l\neq m}^{x,y,z}\beta_{mll}^{2}+\frac{4}{105}\sum_{l\neq m\neq n}^{x,y,z}\beta_{llm}\beta_{mnn}$$

$$+\frac{1}{105}\sum_{l\neq m\neq n}^{x,y,z}\beta_{mll}\beta_{mnn}+\frac{4}{105}\sum_{l\neq m\neq n}^{x,y,z}\beta_{llm}\beta_{nnm}$$

$$+\frac{2}{105}\sum_{l\neq m\neq n}^{x,y,z}\beta_{lmn}^{2}+\frac{4}{105}\sum_{l\neq m\neq n}^{x,y,z}\beta_{lmn}\beta_{mln} \qquad (11)$$

$$\langle\beta_{ZXX}^{2}\rangle=\frac{1}{35}\sum_{l}^{x,y,z}\beta_{lll}^{2}+\frac{4}{105}\sum_{l\neq m}^{x,y,z}\beta_{lll}\beta_{lmm}-\frac{2}{35}\sum_{l\neq m}^{x,y,z}\beta_{llm}\beta_{lmm}+\frac{8}{105}\sum_{l\neq m}^{x,y,z}\beta_{llm}^{2}$$

$$+\frac{3}{35}\sum_{l\neq m}^{x,y,z}\beta_{lmm}^{2}-\frac{2}{35}\sum_{l\neq m}^{x,y,z}\beta_{llm}\beta_{mll}+\frac{1}{35}\sum_{l\neq m\neq n}^{x,y,z}\beta_{lmm}\beta_{lnn}$$

$$-\frac{2}{105}\sum_{l\neq m\neq n}^{x,y,z}\beta_{lln}\beta_{mnn}-\frac{2}{105}\sum_{l\neq m\neq n}^{x,y,z}\beta_{llm}\beta_{mnn}$$

$$+\frac{2}{35}\sum_{l\neq m\neq n}^{x,y,z}\beta_{lmn}^{2}-\frac{2}{105}\sum_{l\neq m\neq n}^{x,y,z}\beta_{lmn}\beta_{lmn} \qquad (12)$$

3.8 Two-Photon Absorption (2PA) Calculations

2PA is a third-order nonlinear process, the simultaneous absorption of two photons of similar energy is called as two photon absorption.[56] The increase in the percentage of the CT nature in a molecule has also reported to increase the 2PA cross-section. The 2PA cross-section is typically determined using the Goppert Mayer (GM) unit. The relationship between the GM and atomic unit is determined by the following equation 13.[57]

$$\delta_{\mathrm{GM}}=\frac{8\pi^{2}\alpha a_{0}^{5}\,\omega_{f}^{2}}{c\Gamma}\,\delta_{\mathrm{au}} \qquad (13)$$

The variables in the **Equation 13** are defined as follows: α represents the fine structure constant, a_0 represents the Bohr radius; c represents the speed of light in a vacuum. The 2PA cross sections obtained for these molecules are large which suggests that the investigated chromophores are promising as new organic materials for NLO. The 2PA cross section obtained for **PPAB-2** (δ^{TP} = 6354 a.u. at 1771 nm) is five times higher than PPAB-3 (δ^{TP} =

1136 a.u. at 1560 nm, see **Table 6**). The two molecules consist of very similar molecular structure but two different lateral donor groups: TPA vs. DPA. Our results indicate that due to the π linker in PPAB-2 is Thienyl whereas in PPAB-3 it is phenylene linker leading to enhanced ICT and consequently larger two-photon absorption in PPAB-2.

Table 6. The two-photon tensor elements of D−π–A framework containing PPAB molecules were computed at the B3LYP/ 6-31G* level of theory in Acetonitrile solvent phase.

Molecules	2PA	S_{xx}	S_{yy}	S_{zz}	S_{xy}	S_{xz}	S_{yz}	δ^{TP} (au)
PPAB-1	1158 nm 1.07 eV	182.4	14.1	1.2	- 56.4	-3.8	0.4	50.64
PPAB-2	1771 nm 0.7 eV	-3360.8	118.5	0.2	708.4	-23.4	-10.4	6354.24
PPAB-3	1,560 nm 0.79 eV	368.0	-1337.0	2.2	-117.1	-2.7	6.1	1136.17

4. CONCLUSION

This study presents quantum chemical investigation of the series of novel ICT-based chromophores with D–π–A configuration consisting of aza-BODIPY framework based pyrrolopyrrole aza-BODIPY (PPAB) as the electron acceptor group, and the triphenylamine (TPA) or diphenylamine (DPA) groups act as the electron donor group. First hyperpolarizability of the studied molecules is found to be strongly dependent on the extent of the charge transfer between the electronic donor and the acceptor group through the π-electron bridge. The effect of functional and basis set on the absorption properties of the D–π–A-–π–D molecules are studied to determine the best suitable functional/ basis set combination for studies of NLO response. The first hyperpolarizability of D–π–A molecules is significantly higher than the reference molecule p-Nitroanline, indicating suitability of these molecules for further exploration for designing NLO materials. The Second-order non-linear polarizability β_{HRS} is calculated at 1064 nm in Acetonitrile. Our results indicate that NLO response of novel ICT chromophores could be optimized through rational design by the use of suitable donor, acceptor and π-linkers that give rise to unidirectional charge transfer. The 2PA cross-section can also be significantly enhanced through careful modification of the donor and the linker substituents. These results indicate that the present study could serve as basis for studies of second and third-order NLO properties of ICT-based chromophores

consisting of PPAB electronic acceptor with suitable electronic donor and π-linkers with D–π–A framework for future technological applications.

Supplementary Materials

The supplementary material contains absorption data comparison using different functionals with the experimental provided data for **:** D–π–A-π–D framework containing molecules along with values of μ, α_{av}, β_{total} and β_{vec}, obtained using the ω*B97XD tuned functional and 6-31g* basis set, HOMO-LUMO energies of the PPAB molecules in different solvents with varying polarity and the electron density images of the molecules. (PDF)

Acknowledgements

N.P.S.K. thanks GITAM for research fellowship. R.M. acknowledges Prof. P. Hegemann for constant encouragements. We acknowledge high performance computing (HPC) facility and storage resources at GITAM.

ORCID

Naga Pranava Sree Kothoori: 0009-0005-9550-5013

Pandiyan Sivasakthi: 0000-0001-8542-2904

Mallesham Baithy: 0000-0003-2184-837X

Ramprasad Misra: 0000-0002-1599-404X

Pralok K. Samanta: 0000-0002-1926-7720

Conflicts of Interest

The authors declare no competing financial interest

References:

(1) Yu, J.; Luo, M.; Lv, Z.; Huang, S.; Hsu, H. H.; Kuo, C. C.; Han, S. T.; Zhou, Y. Recent Advances in Optical and Optoelectronic Data Storage Based on Luminescent Nanomaterials. *Nanoscale* **2020**, *12* (46), 23391–23423.

(2) Dalton, L. R.; Sullivan, P. A.; Bale, D. H. Electric Field Poled Organic Electro-Optic Materials: State of the Art and Future Prospects. *Chem. Rev.* **2010**, *110* (1), 25–55.

(3) Yang, L.; El-Tamer, A.; Hinze, U.; Li, J.; Hu, Y.; Huang, W.; Chu, J.; Chichkov, B. N. Two-Photon Polymerization of Cylinder Microstructures by Femtosecond Bessel Beams. *Appl. Phys. Lett.* **2014**, *105* (4).

(4) Khalid, M.; Lodhi, H. M.; Khan, M. U.; Imran, M. Structural Parameter-Modulated Nonlinear Optical Amplitude of Acceptor-π-D-π-Donor-Configured Pyrene Derivatives: A DFT Approach. *RSC Adv.* **2021**, *11* (23), 14237–14250.

(5) Feng, Q.; Li, Y.; Shi, G.; Wang, L.; Zhang, W.; Li, K.; Hou, H.; Song, Y. A Photo-Controllable Third-Order Nonlinear Optical (NLO) Switch Based on a Rhodamine B Salicylaldehyde Hydrazone Metal Complex. *J. Mater. Chem. C* **2016**, *4* (36), 8552–8558.

(6) He, G. S.; Lin, T. C.; Prasad, P. N.; Cho, C. C.; Yu, L. J. Optical Power Limiting and Stabilization Using a Two-Photon Absorbing Neat Liquid Crystal in Isotropic Phase. *Appl. Phys. Lett.* **2003**, *82* (26), 4717–4719.

(7) Ivanova, B. B.; Spiteller, M. Possible Application of the Organic Barbiturates as NLO Materials. *Cryst. Growth Des.* **2010**, *10* (6), 2470–2474.

(8) Koos, C.; Vorreau, P.; Vallaitis, T.; Dumon, P.; Bogaerts, W.; Baets, R.; Esembeson, B.; Biaggio, I.; Michinobu, T.; Diederich, F.; Freude, W.; Leuthold, J. All-Optical High-Speed Signal Processing with Silicon-Organic Hybrid Slot Waveguides. *Nat. Photonics* **2009**, *3* (4), 216–219.

(9) De Vega, L.; Van Cleuvenbergen, S.; Depotter, G.; García-Frutos, E. M.; Gómez-Lor, B.; Omenat, A.; Tejedor, R. M.; Serrano, J. L.; Hennrich, G.; Clays, K. Nonlinear Optical Thin Film Device from a Chiral Octopolar Phenylacetylene Liquid Crystal. *J. Org. Chem.* **2012**, *77* (23), 10891–10896.

(10) Maidur, S. R.; Patil, P. S.; Ekbote, A.; Chia, T. S.; Quah, C. K. Molecular Structure, Second- and Third-Order Nonlinear Optical Properties and DFT Studies of a Novel Non-Centrosymmetric Chalcone Derivative: (2E)-3-(4-Fluorophenyl)-1-(4-{[(1E)-(4-Fluorophenyl)Methylene]Amino}phenyl)Prop-2-En-1-One. *Spectrochim. Acta - Part A Mol. Biomol. Spectrosc.* **2017**, *184*, 342–354.

(11) Qian, G.; Wang, Z. Y. Near-Infrared Organic Compounds and Emerging Applications. *Chem. - An Asian J.* **2010**, *5* (5), 1006–1029.

(12) Marques Dos Santos, J.; Jagadamma, L. K.; Latif, N. M.; Ruseckas, A.; Samuel, I. D. W.; Cooke, G. BODIPY Derivatives with near Infra-Red Absorption as Small Molecule Donors for Bulk Heterojunction Solar Cells. *RSC Adv.* **2019**, *9* (27), 15410–15423.

(13) Loudet, A.; Burgess, K. BODIPY Dyes and Their Derivatives: Syntheses and Spectroscopic Properties. *Chem. Rev.* **2007**, *107* (11), 4891–4932.

(14) Bañuelos, J. BODIPY Dye, the Most Versatile Fluorophore Ever? *Chem. Rec.* **2016**, *16* (1), 335–348.

(15) Feng, R.; Sato, N.; Nomura, M.; Saeki, A.; Nakanotani, H.; Adachi, C.; Yasuda, T.; Furuta, H.; Shimizu, S. Near-Infrared Absorbing Pyrrolopyrrole Aza-BODIPY-Based Donor-Acceptor Polymers with Reasonable Photoresponse. *J. Mater. Chem. C* **2020**, *8*

(26), 8770–8776.

(16) Ntziachristos, V.; Ripoll, J.; Weissleder, R. Would Near-Infrared Fluorescence Signals Propagate through Large Human Organs for Clinical Studies? *Opt. Lett.* **2002**, *27* (5), 333.

(17) Russier-Antoine, I.; Bertorelle, F.; Calin, N.; Sanader, Ž.; Krstić, M.; Comby-Zerbino, C.; Dugourd, P.; Brevet, P. F.; Bonacic-Koutecky, V.; Antoine, R. Ligand-Core NLO-Phores: A Combined Experimental and Theoretical Approach to the Two-Photon Absorption and Two-Photon Excited Emission Properties of Small-Ligated Silver Nanoclusters. *Nanoscale* **2017**, *9* (3), 1221–1228.

(18) Samanta, P. K.; Alam, M. M.; Misra, R.; Pati, S. K. Tuning of Hyperpolarizability, and One- and Two-Photon Absorption of Donor-Acceptor and Donor-Acceptor-Acceptor-Type Intramolecular Charge Transfer-Based Sensors. *Phys. Chem. Chem. Phys.* **2019**, *21* (31), 17343–17355.

(19) Kanis, D. R.; Ratner, M. A.; Marks, T. J. Design and Construction of Molecular Assemblies with Large Second-Order Optical Nonlinearities. Quantum Chemical Aspects. *Chem. Rev.* **1994**, *94* (1), 195–242.

(20) Zojer, E.; Beljonne, D.; Pacher, P.; Brédas, J. L. Two-Photon Absorption in Quadrupolar π-Conjugated Molecules: Influence of the Nature of the Conjugated Bridge and the Donor-Acceptor Separation. *Chem. - A Eur. J.* **2004**, *10* (11), 2668–2680.

(21) Lee, W. H.; Lee, H.; Kim, J. A.; Choi, J. H.; Cho, M.; Jeon, S. J.; Cho, B. R. Two-Photon Absorption and Nonlinear Optical Properties of Octupolar Molecules. *J. Am. Chem. Soc.* **2001**, *123* (43), 10658–10667.

(22) Wang, Y.; Mori, S.; Nakanotani, H.; Adachi, C.; Shimizu, S. Post-Modification of Pyrrolopyrrole Aza-BODIPY toward High Near-Infrared Fluorescence Brightness. *Org. Lett.* **2023**, *25* (17), 3040–3044.

(23) Schäfer, C.; Mony, J.; Olsson, T.; Börjesson, K. Effect of the Aza-N-Bridge and Push-Pull Moieties: A Comparative Study between BODIPYs and Aza-BODIPYs. *J. Org. Chem.* **2022**, *87* (5), 2569–2579.

(24) Akemann, W.; Laage, D.; Plaza, P.; Martin, M. M.; Blanchard-Desce, M. Photoinduced Intramolecular Charge Transfer in Push-Pull Polyenes: Effects of Solvation, Electron-Donor Group, and Polyenic Chain Length. *J. Phys. Chem. B* **2008**, *112* (2), 358–368.

(25) Muhammad, S.; Xu, H.; Su, Z. Capturing a Synergistic Effect of a Conical Push and an Inward Pull in Fluoro Derivatives of Li@B10H14 Basket: Toward a Higher Vertical Ionization Potential and Nonlinear Optical Response. *J. Phys. Chem. A* **2011**, *115* (5), 923–931.

(26) Mao, G. J.; Wei, T. T.; Wang, X. X.; Huan, S. Y.; Lu, D. Q.; Zhang, J.; Zhang, X. B.; Tan, W.; Shen, G. L.; Yu, R. Q. High-Sensitivity Naphthalene-Based Two-Photon Fluorescent Probe Suitable for Direct Bioimaging of H2S in Living Cells. *Anal. Chem.* **2013**, *85* (16), 7875–7881.

(27) Kim, D.; Ryu, H. G.; Ahn, K. H. Recent Development of Two-Photon Fluorescent Probes for Bioimaging. *Org. Biomol. Chem.* **2014**, *12* (26), 4550–4566.

(28) Feng, L. L.; Wu, Y. X.; Zhang, D. L.; Hu, X. X.; Zhang, J.; Wang, P.; Song, Z. L.; Zhang, X. B.; Tan, W. Near Infrared Graphene Quantum Dots-Based Two-Photon Nanoprobe for Direct Bioimaging of Endogenous Ascorbic Acid in Living Cells. *Anal. Chem.* **2017**, *89* (7), 4077–4084.

(29) Bouit, P. A.; Kamada, K.; Feneyrou, P.; Berginc, G.; Toupet, L.; Maury, O.; Andraud, C. Two-Photon Absorption-Related Properties of Functionalized Bodipy Dyes in the Infrared Range up to Telecommunication Wavelengths. *Adv. Mater.* **2009**, *21* (10–11), 1151–1154.

(30) Bokareva, O. S.; Grell, G.; Bokarev, S. I.; Kühn, O. Tuning Range-Separated Density Functional Theory for Photocatalytic Water Splitting Systems. *J. Chem. Theory Comput.* **2015**, *11* (4), 1700–1709.

(31) Kronik, L.; Stein, T.; Refaely-Abramson, S.; Baer, R. Excitation Gaps of Finite-Sized Systems from Optimally Tuned Range-Separated Hybrid Functionals. *J. Chem. Theory Comput.* **2012**, *8* (5), 1515–1531.

(32) M. J. Frisch, G. W. Trucks, H. B. Schlegel, G. E. S.; M. A. Robb, J. R. Cheeseman, G. Scalmani, V. B.; G. A. Petersson, H. Nakatsuji, X. Li, M. Caricato, A. V. M.; J. Bloino, B. G. Janesko, R. Gomperts, B. Mennucci, H. P. H.; J. V. Ortiz, A. F. Izmaylov, J. L. Sonnenberg, D. W.-Y.; F. Ding, F. Lipparini, F. Egidi, J. Goings, B. Peng, A. P.; T. Henderson, D. Ranasinghe, V. G. Zakrzewski, J. Gao, N. R.; G. Zheng, W. Liang, M. Hada, M. Ehara, K. Toyota, R. F.; J. Hasegawa, M. Ishida, T. Nakajima, Y. Honda, O. Kitao, H. N.; T. Vreven, K. Throssell, J. A. Montgomery, Jr., J. E. P.; F. Ogliaro, M. J. Bearpark, J. J. Heyd, E. N. Brothers, K. N. K.; V. N. Staroverov, T. A. Keith, R. Kobayashi, J. N.; K. Raghavachari, A. P. Rendell, J. C. Burant, S. S. I.; J. Tomasi, M. Cossi, J. M. Millam, M. Klene, C. Adamo, R. C.; J. W. Ochterski, R. L. Martin, K. Morokuma, O. F.; J. B. Foresman, and D. J. F. Gaussian 16, Revision C.02. *Gaussian, Inc. Wallingford CT* **2019**.

(33) Marenich, A. V.; Cramer, C. J.; Truhlar, D. G. Universal Solvation Model Based on Solute Electron Density and on a Continuum Model of the Solvent Defined by the Bulk Dielectric Constant and Atomic Surface Tensions. *J. Phys. Chem. B* **2009**, *113* (18), 6378–6396.

(34) Kara Zaitri, L.; Mekelleche, S. M. Computational Study of Linear and Nonlinear Optical Properties of Substituted Thiophene Imino Dyes Using Long-Range Corrected Hybrid DFT Methods. *Mol. Phys.* **2020**, *118* (4).

(35) Humphrey, W.; Dalke, A.; Schulten, K. VMD: Visual Molecular Dynamics. *J. Mol. Graph.* **1996**, *14* (1), 33–38.

(36) Lu, T.; Chen, F. Multiwfn: A Multifunctional Wavefunction Analyzer. *J. Comput. Chem.* **2012**, *33* (5), 580–592.

(37) Aidas, K.; Angeli, C.; Bak, K. L.; Bakken, V.; Bast, R.; Boman, L.; Christiansen, O.; Cimiraglia, R.; Coriani, S.; Dahle, P.; Dalskov, E. K.; Ekström, U.; Enevoldsen, T.; Eriksen, J. J.; Ettenhuber, P.; Fernández, B.; Ferrighi, L.; Fliegl, H.; Frediani, L.; Hald, K.; Halkier, A.; Hättig, C.; Heiberg, H.; Helgaker, T.; Hennum, A. C.; Hettema, H.; Hjertenæs, E.; Høst, S.; Høyvik, I. M.; Iozzi, M. F.; Jansík, B.; Jensen, H. J. A.; Jonsson, D.; Jørgensen, P.; Kauczor, J.; Kirpekar, S.; Kjærgaard, T.; Klopper, W.; Knecht, S.; Kobayashi, R.; Koch, H.; Kongsted, J.; Krapp, A.; Kristensen, K.; Ligabue, A.; Lutnæs, O. B.; Melo, J. I.; Mikkelsen, K. V.; Myhre, R. H.; Neiss, C.; Nielsen, C. B.; Norman, P.; Olsen, J.; Olsen, J. M. H.; Osted, A.; Packer, M. J.; Pawlowski, F.;

Pedersen, T. B.; Provasi, P. F.; Reine, S.; Rinkevicius, Z.; Ruden, T. A.; Ruud, K.; Rybkin, V. V.; Sałek, P.; Samson, C. C. M.; de Merás, A. S.; Saue, T.; Sauer, S. P. A.; Schimmelpfennig, B.; Sneskov, K.; Steindal, A. H.; Sylvester-Hvid, K. O.; Taylor, P. R.; Teale, A. M.; Tellgren, E. I.; Tew, D. P.; Thorvaldsen, A. J.; Thøgersen, L.; Vahtras, O.; Watson, M. A.; Wilson, D. J. D.; Ziolkowski, M.; Ågren, H. The Dalton Quantum Chemistry Program System. *Wiley Interdiscip. Rev. Comput. Mol. Sci.* **2014**, *4* (3), 269–284.

(38) Cammi, R.; Mennucci, B.; Tomasi, J. Solvent Effects on Linear and Nonlinear Optical Properties of Donor- Acceptor Polyenes: Investigation of Electronic and Vibrational Components in Terms of Structure and Charge Distribution Changes. *J. Am. Chem. Soc.* **1998**, *120* (34), 8834–8847.

(39) Khalid, M.; Ali, A.; Jawaria, R.; Asghar, M. A.; Asim, S.; Khan, M. U.; Hussain, R.; Fayyaz ur Rehman, M.; Ennis, C. J.; Akram, M. S. First Principles Study of Electronic and Nonlinear Optical Properties of A-D-π-A and D-A-D-π-A Configured Compounds Containing Novel Quinoline-Carbazole Derivatives. *RSC Adv.* **2020**, *10* (37), 22273–22283.

(40) Jia, J.; Wu, X.; Zhang, X.; Wang, Y.; Yang, J.; Fang, Y.; Song, Y. Effect of Intramolecular Charge Transfer on Nonlinear Optical Properties of Chalcone Derivatives: A Visual Description of the Charge Transfer Process. *Phys. Chem. Chem. Phys.* **2022**, *24* (2), 955–965.

(41) Fukui, K. Role of Frontier Orbitals in Chemical Reactions. *Science* **1982**, *218* (4574), 747–754.

(42) Koopmans, T. Über Die Zuordnung von Wellenfunktionen Und Eigenwerten Zu Den Einzelnen Elektronen Eines Atoms. *Physica* **1934**, *1* (1–6), 104–113.

(43) Parr, R. G.; Pearson, R. G. Absolute Hardness: Companion Parameter to Absolute Electronegativity. *J. Am. Chem. Soc.* **1983**, *105* (26), 7512–7516.

(44) Plaquet, A.; Bogdan, E.; Antonov, L.; Rodriguez, V.; Ducasse, L.; Champagne, B.; Castet, F. Solvent Effects on the Nonlinear Optical Responses of Anil Derivatives. *AIP Conf. Proc.* **2015**, *1642*, 488–496.

(45) Aggarwal, N.; Patnaik, A. A New Class of Nitroanilinic Dimer, the PNA O-Dimer: Electronic Structure and Emission Characteristics of O-Dimeric Aggregates. *J. Phys. Chem. A* **2015**, *119* (30), 8388–8399.

(46) Hernández-Paredes, J.; Glossman-Mitnik, D.; Duarte-Moller, A.; Flores-Holguín, N. Theoretical Calculations of Molecular Dipole Moment, Polarizability, and First Hyperpolarizability of Glycine-Sodium Nitrate. *J. Mol. Struct. THEOCHEM* **2009**, *905* (1–3), 76–80.

(47) Kleinman, D. A. Nonlinear Dielectric Polarization in Optical Media. *Phys. Rev.* **1962**, *126* (6), 1977–1979.

(48) Misra, R. Tuning of Second-Order Nonlinear Optical Response Properties of Aryl-Substituted Boron-Dipyrromethene Dyes: Unidirectional Charge Transfer Coupled with Structural Tailoring. *J. Phys. Chem. C* **2017**, *121* (10), 5731–5739.

(49) Misra, R.; Bhattacharyya, S. P. Medium Effect on ICT Process: Theory and Experiments . *Intramol. Charg. Transf.* **2018**, 115–148.

(50) Das, P. K. Chemical Applications of Hyper-Rayleigh Scattering in Solution. *J. Phys. Chem. B* **2006**, *110* (15), 7621–7630.

(51) Yao, Y.; Xu, H. L.; Su, Z. M. Switching of Second-Order Nonlinear Response Effected by Different Acceptors: The Impacts of Environment and Frequency Dispersion. *Dye. Pigment.* **2021**, *193*, 109502.

(52) Milne, B. F.; Nogueira, F.; Cardoso, C. Theoretical Study of Heavy-Atom Tuning of Nonlinear Optical Properties in Group 15 Derivatives of N,N,N-Trimethylglycine (Betaine). *Dalt. Trans.* **2013**, *42* (10), 3695–3703.

(53) Castet, F.; Bogdan, E.; Plaquet, A.; Ducasse, L.; Champagne, B.; Rodriguez, V. Reference Molecules for Nonlinear Optics: A Joint Experimental and Theoretical Investigation. *J. Chem. Phys.* **2012**, *136,* 024506.

(54) Rice, J. E.; Amos, R. D.; Colwell, S. M.; Handy, N. C.; Sanz, J. Frequency Dependent Hyperpolarizabilities with Application to Formaldehyde and Methyl Fluoride. *J. Chem. Phys.* **1990**, *93* (12), 8828–8839.

(55) Mançois, F.; Sanguinet, L.; Pozzo, J. L.; Guillaume, M.; Champagne, B.; Rodriguez, V.; Adamietz, F.; Ducasse, L.; Castet, F. Acido-Triggered Nonlinear Optical Switches: Benzazolo-Oxazolidines. *J. Phys. Chem. B* **2007**, *111* (33), 9795–9802.

(56) Beverina, L.; Fu, J.; Leclercq, A.; Zojer, E.; Pacher, P.; Barlow, S.; Van Stryland, E. W.; Hagan, D. J.; Brédas, J. L.; Marder, S. R. Two-Photon Absorption at Telecommunications Wavelengths in a Dipolar Chromophore with a Pyrrole Auxiliary Donor and Thiazole Auxiliary Acceptor. *J. Am. Chem. Soc.* **2005**, *127* (20), 7282–7283.

(57) Arul Murugan, N.; Kongsted, J.; Rinkevicius, Z.; Aidas, K.; Mikkelsen, K. V.; Ågren, H. Hybrid Density Functional Theory/Molecular Mechanics Calculations of Two-Photon Absorption of Dimethylamino Nitro Stilbene in Solution. *Phys. Chem. Chem. Phys.* **2011**, *13* (27), 12506–12516.